The American Journal of Pathology, Vol. 170, No. 1, January 2007
Copyright © American Society for Investigative Pathology
DOI: 10.2353/ajpath.2007.060406

Vascular Biology, Atherosclerosis and Endothelium Biology

Complement C1q Reduces Early Atherosclerosis in Low-Density Lipoprotein Receptor-Deficient Mice

Vinay K. Bhatia,* Sheng Yun,*† Viola Leung,*† David C. Grimsditch,‡ G. Martin Benson,‡ Marina B. Botto,§ Joseph J. Boyle,† and Dorian O. Haskard*

From the British Heart Foundation Cardiovascular Medicine Unit, Vascular Science Section, National Heart and Lung Institute, Imperial College, London; Department of Histopathology,† Hammersmith Hospital, London; Atherosclerosis Department,‡ GlaxoSmithKline, Stevenage; and Rheumatology Unit,§ Division of Medicine, Imperial College, London, United Kingdom*

We explored the role of the classic complement pathway in atherogenesis by intercrossing C1q-deficient mice (*C1qa*$^{-/-}$) with low-density lipoprotein receptor knockout mice (*Ldlr*$^{-/-}$). Mice were fed a normal rodent diet until 22 weeks of age. Aortic root lesions were threefold larger in *C1qa*$^{-/-}$/*Ldlr*$^{-/-}$ mice compared with *Ldlr*$^{-/-}$ mice (3.72 ± 1.0% aortic root versus 1.1 ± 0.4%; mean ± SEM, $P < 0.001$). Furthermore, the cellular composition of lesions in *C1qa*$^{-/-}$/*Ldlr*$^{-/-}$ was more complex, with an increase in vascular smooth muscle cells. The greater aortic root lesion size in *C1qa*$^{-/-}$/*Ldlr*$^{-/-}$ mice occurred despite a significant reduction in C5b-9 deposition per lesion unit area, suggesting the critical importance of proximal pathway activity. Apoptotic cells were readily detectable by cleaved caspase-3 staining, terminal deoxynucleotidyl transferase dUTP nick-end labeling assay, and electron microscopy in *C1qa*$^{-/-}$/*Ldlr*$^{-/-}$, whereas apoptotic cells were not detected in *Ldlr*$^{-/-}$ mice. This is the first direct demonstration of a role for the classic complement pathway in atherogenesis. The greater lesion size in *C1qa*$^{-/-}$/*Ldlr*$^{-/-}$ mice is consistent with the emerging homeostatic role for C1q in the disposal of dying cells. This study suggests the importance of effective apoptotic cell removal for containing the size and complexity of early lesions in atherosclerosis. *(Am J Pathol 2007, 170:416–426; DOI: 10.2353/ajpath.2007.060406)*

The complement system contains a family of proteins that provides an important arm of the innate immune system.[1,2] Complement can be activated via the classic, alternative, or mannose-binding lectin (MBL) pathways, each of which converges on C3, the central hub of the complement system. Activation of C3 generates leukocyte chemoattractants C3a and C5a and the assembly of terminal complement complexes (C5b-7, C5b-8, C5b-9), which insert into cell membranes and cause cell lysis or activation.[3] However, not all effects of complement activation are proinflammatory, since upstream complement components (C1q, MBL, C3bi) may facilitate the clearance of apoptotic cells and other debris.[4–6]

Programed cell death (apoptosis) is a feature of human atherosclerosis and is associated with development of the lesion necrotic core as well as instability of complex plaques.[7–9] Stimuli that trigger macrophage apoptosis include ingestion of free cholesterol and oxidized low-density lipoprotein (LDL).[10–12] On the other hand, vascular smooth muscle cell (VSMC) apoptosis may be stimulated by modified LDL, tumor necrosis factor α, and other cytokines, or by surface contact interactions with activated macrophages.[13–15] Apoptotic cells are often detectable in late atherosclerotic lesions but are not usually identified in early lesions, in large part due to highly efficient removal of apoptotic cells by macrophages and also, possibly, a more proapoptotic environment in advanced lesions.[16,17]

Complement C1q initiates activation of the classic pathway, typically through binding immunoglobulin Fc in immune complexes. However, C1q also binds apoptotic cells and plays an important role in their disposal.[18–21] The mechanism underlying C1q-mediated clearance of apoptotic cells is unclear but is likely to involve calreticulin and CD91-dependent docking of C1q on phagocytes.[22] In this study, we have used C1q gene-targeted mice to test the hypothesis that the classic complement pathway plays a role in apoptotic cell clearance in ath-

Funded by the British Heart Foundation and Hammersmith Hospital Trust Research Committee.

S.Y. and V.L. contributed equally to this work.

Accepted for publication October 10, 2006.

Address reprint requests to Prof. Dorian O. Haskard, BHF Cardiovascular Medicine Unit, Hammersmith Hospital, Du Cane Road, London, W12 0NN UK. E-mail: d.haskard@imperial.ac.uk.

erosclerosis and that defective apoptotic cell clearance increases lesion development.

Materials and Methods

Reagents

Oil Red O, dextrin, gelatin, Mayer's hematoxylin, L-glutamic acid, glycerol, sodium azide, calcium chloride, magnesium sulfate, and sodium phosphate were obtained from Merck/BDH, Poole, UK. Buffered formal saline (2% formaldehyde in phosphate-buffered saline) was from Pioneer Research Chemicals, Colchester, Essex, UK. OCT compound was from CellPath, Newtown, Powys, UK. Other reagents were from Sigma, St. Louis, MO.

Mice

C1q gene-targeted mice (*C1qa*$^{-/-}$) were generated in-house.[23] *Ldlr*$^{-/-}$ mice were obtained from Jackson Laboratories (Bar Harbor, ME). Both *C1qa*$^{-/-}$ and *Ldlr*$^{-/-}$ mice were backcrossed for 10 generations onto the C57BL/6 background before intercrossing to form *C1qa*$^{-/-}$/*Ldlr*$^{-/-}$ double knockout mice. Mice genotypes were determined by polymerase chain reaction. All mice in the study were female. We conducted two separate experiments using mice fed a normal laboratory diet. In the first, 14 *Ldlr*$^{-/-}$ and 19 *C1qa*$^{-/-}$/*Ldlr*$^{-/-}$ mice were analyzed for serum lipids, lipoprotein profiles, serum autoantibodies, and aortic root lesion area. In the second, 19 *Ldlr*$^{-/-}$ and eight *C1qa*$^{-/-}$/*Ldlr*$^{-/-}$ mice were assessed for aortic root lesion area and cellular composition of lesions. A further experiment was conducted in which 10 *Ldlr*$^{-/-}$ and 10 *C1qa*$^{-/-}$/*Ldlr*$^{-/-}$ mice were fed a cholate-free high-fat diet (Diet W; Hope Farms, Woerden, The Netherlands) consisting of (w/w) cocoa butter (15%), cholesterol (0.25%), sucrose (40.5%), cornstarch (10%), corn oil (1%), cellulose (5.95%), casein (20%), 50% choline chloride (2%), methionine (0.2%), and mineral mixture (5.1%) These mice were gradually transferred onto the high-fat diet at 10 weeks of age and sacrificed at 22 weeks of age. Animals were housed in a specific pathogen-free environment and studied according to UK Home Office regulations. Urinary protein was determined using Hema-combistick (Bayler plc, Newbury, Berks, UK).

Lipoprotein, Cholesterol, and Triglyceride Analysis

Terminal blood was collected in Microvette CB-300 blood tubes (Sarstedt, Nümbrecht, Germany) and allowed to clot at 4°C. Serum was pooled from all mice in the same group and kept at 4°C for up to 24 hours before analysis. Lipoprotein profiles were analyzed on pooled sera by size-exclusion chromatography using a SMART micro-FPLC system (Pharmacia, Stockholm, Sweden).[24] Total cholesterol was measured enzymatically on each individual mouse using Kit CII (no. 270-54399/54499) from Wako Chemicals, GmbH, Neuss, Germany. Serum triglycerides were measured enzymatically using a kit purchased from ABX Diagnostics, Montpellier, France.

Autoimmune Serology

Antibodies to single-stranded DNA (ssDNA) were measured by enzyme-linked immunosorbent assay.[25] The levels of IgM and IgG autoantibody titers to malondialdehyde-LDL and copper-oxidized LDL were determined in serum from individual mice in the laboratory of Dr. Joseph Witztum at the University of California, San Diego, in La Jolla, CA, using previously described methods.[26]

Aortic Root Histology

Hearts and aortae were perfused *in situ* with oxygenated Krebs-Henseleit buffer at 37°C under a pressure of ~110 cm water via a cannula inserted in the left ventricle and an outlet created by incision of the right atrium. After 30 minutes, the buffer was replaced with 2% buffered formal saline at 37°C for a further 30 minutes. The heart, aortae, liver, and kidneys were then removed and stored in 2% formal saline. Cryosections of the aortic root were taken as previously described.[27,28] For each mouse, the entire aortic root from where the three valve leaflets first appeared was serially sectioned into 5-μm sections, and every 10th section (50 μm) was stained with Oil Red O and counterstained with Mayer's hematoxylin.

Lesion Quantification

Aortic root sections were coded and analyzed blind. Sections were imaged using an Olympus BH-2 microscope (Tokyo, Japan) equipped with ×4 objective (total magnification ×40), three neutral density filters (2× ND-6 and 1× ND-25), and a video camera (HV-C10; Hitachi, Yokohama, Japan). Twenty-four-bit color images were acquired and analyzed using a PC (Datacell Pentium P5-133; Datacell, Berks, UK) fitted with a framegrabbing board (IC-PCI; Imaging Technologies, Bedford, MA) and Optimas software (version 6.1; Optimas Corp., Bothell, WA). The images were captured under identical lighting, microscope, camera, and PC conditions. Quantification was performed by drawing around the lesions and the aortic wall using the Image ProPlus software (version 4.5; Media Cybernetics, Silver Spring, MD). Absolute values for cross-sectional area were obtained by calibrating the software using an image of a micrometer slide taken at the same magnification. The individual lesion areas per aortic root section of each mouse were averaged to obtain the mean lesion area per mouse. The lesion area fraction was calculated by dividing the mean lesion area by the mean area of the aortic wall and expressed as a percentage, as previously described.[29]

Immunohistochemistry

Immunohistochemistry was performed by standard procedures on residual sections not required for analysis of

Table 1. Body Weights and Total Serum Cholesterol and Triglycerides in 22-Week-Old C57BL/6 *Ldlr*$^{-/-}$ and *C1qa*$^{-/-}$/*Ldlr*$^{-/-}$

Mouse strain	Diet	*n*	Final body weight (g) (mean ± SD)	Total cholesterol (mmol/L) (mean ± SD)	Triglyceride (mmol/L) (mean ± SD)
Ldlr$^{-/-}$	Normal	14	24 ± 2	8.56 ± 1.03	1.89 ± 0.56
C1qa$^{-/-}$/*Ldlr*$^{-/-}$	Normal	19	25 ± 2	8.97 ± 1.63	2.10 ± 0.54
Ldlr$^{-/-}$	High fat	10	25 ± 3	25.60 ± 5.84	3.02 ± 1.00
C1qa$^{-/-}$/*Ldlr*$^{-/-}$	High fat	10	25 ± 3	30.66 ± 6.42	3.74 ± 1.02

lesion size. We phenotyped lesions for macrophages (Moma-2; Serotec, Oxford, UK) and smooth muscle cell α-actin (clone α-1-A4; Sigma-Aldrich, Poole, UK), detecting positive cells with alkaline phosphatase and Vector Blue. Other primary antibodies used were against B lymphocytes (CD19; Pharmingen, Oxford, UK), T lymphocytes (CD3; Pharmingen), IgM (Abcam, Cambridge, UK), IgG (biotinylated anti-mouse IgG Vector), C3 (anti-mouse C3; MP Biomedicals, London, UK), and rabbit anti-C5b-9 (Calbiochem, Merck Biosciences, Darmstadt, Germany) and were detected with avidin-biotin peroxidase (Dako, Ely, UK) and diaminobenzidine (DAB) substrate (brown).

Anti-C5b-9 Immunodetection

Anti-C5b-9 was titrated in doubling dilutions on atherosclerotic sections, using a standard avidin-biotin-peroxidase-DAB detection layer. Then, anti-C5b-9 was diluted to working concentration in normal human serum or in C3-deficient human serum (Sigma). C5b-9-coated beads for adsorption of anti-C5b-9 antibodies were prepared by mixing polystyrene beads (no. 17136; Polysciences, Warrington, PA) 1:1 with 1 mg/ml IgM solution (The Binding Site, Birmingham, UK) at 4°C for 24 hours. The beads were washed once in phosphate-buffered saline (PBS) by centrifugation and resuspension and then added to the anti-C5b-9 antibodies in sera. As a complement-fixing immunoglobulin, IgM activates C5b-9 generation in normal serum but not C3-deficient serum. The beads were incubated for 120 minutes at 37°C and then removed by centrifugation. The supernatants were added to tissue sections, and immunostaining was performed as above.

Detection of Apoptotic Cells

Apoptotic cells were detected by immunostaining with a rabbit antibody to an epitope on caspase-3 (1 μg/ml Clone CM1; Becton, Dickinson and Company, Oxford, UK) that is revealed in cells undergoing apoptosis and detected with biotinylated swine anti-rabbit (Dako), avidin-biotin peroxidase (Dako), and DAB substrate. Terminal deoxynucleotidyl transferase dUTP nick-end labeling (TUNEL) staining was performed using each of two kits (Roche, Welwyn Garden City, UK; and Oncogene Sciences, Gaithersburg, MD) according to the manufacturer's instructions. These enzymatically incorporate fluoresceinated nucleotides into (broken) DNA ends. Peroxidase conversion with peroxidase-labeled anti-fluorescein antibodies and DAB were used to give a stable brown product. For each kit, the TUNEL incubation time was carefully titrated on positive control sections to optimize staining intensity. The TUNEL indices obtained with each kit were closely correlated (Spearman's correlation coefficient = 0.95). Results of immunocytochemistry are presented as a percentage area fraction of the aortic root or as the percentage of lesional cells.

Confocal Microscopy

Confocal immunostaining and microscopy was by modification of routine immunohistochemistry, primarily substituting fluorescent antibodies for the peroxidase second layers and TOPRO-3 for hematoxylin. In brief, cryostat sections were blocked in 10% normal goat serum (Dako) and incubated with antibodies to Moma-2 and/or smooth muscle actin (as above). Sections were washed briefly in PBS and then incubated in 1:200 goat-anti-rat-AlexaFluor 488 (Molecular Probes, Eugene, OR). Anti-activated caspase-3 immunostaining was performed with anti-cleaved caspase-3 epitope, as above, but detected with goat-anti-rabbit-AlexaFluor 488 (Molecular Probes). TUNEL was performed with the Roche kit (as above) under the same conditions but was stopped after incorporation of the fluoresceinated thymidine. For use with TUNEL and anti-cleaved caspase-3, Moma-2 staining was visualized with goat anti-rat AlexaFluor 568 or AlexaFluor 546 (which are spectrally similar). Throughout, after the second layer, sections were washed briefly in PBS and then incubated 10 minutes with TOPRO-3 (Molecular Probes), rinsed in PBS, and mounted in PBS/glycerol. Staining and storage were in the dark as much as practicable. Sections were examined with a Zeiss LSM 510 Meta inverted confocal microscope (Carl Zeiss GmbH, Jena, Germany), illuminated using Argon 488, HeNe 543, and HeNe 633 lines. Pinhole and tunable filter settings were at defaults for the objectives and the fluorescein isothiocyanate (FITC)/Cy3/Cy5MT wavelengths. Scan and photomultiplier settings were set to optimize signal/noise ratio for each emission wavelength. Processing was conducted with a Zeiss LSM Image Browser and comprised the addition of scale bars and adjustment of brightness and contrast before import into Microsoft Powerpoint (Redmond, WA) for assembly of montage figures.

Electron Microscopy

One parallel cryostat section was selected from each of four *C1qa*$^{-/-}$/*Ldlr*$^{-/-}$ mice to correspond closely to those used for the confocal analysis of double immunostaining of Moma-2 and cleaved caspase-3 or TUNEL. These

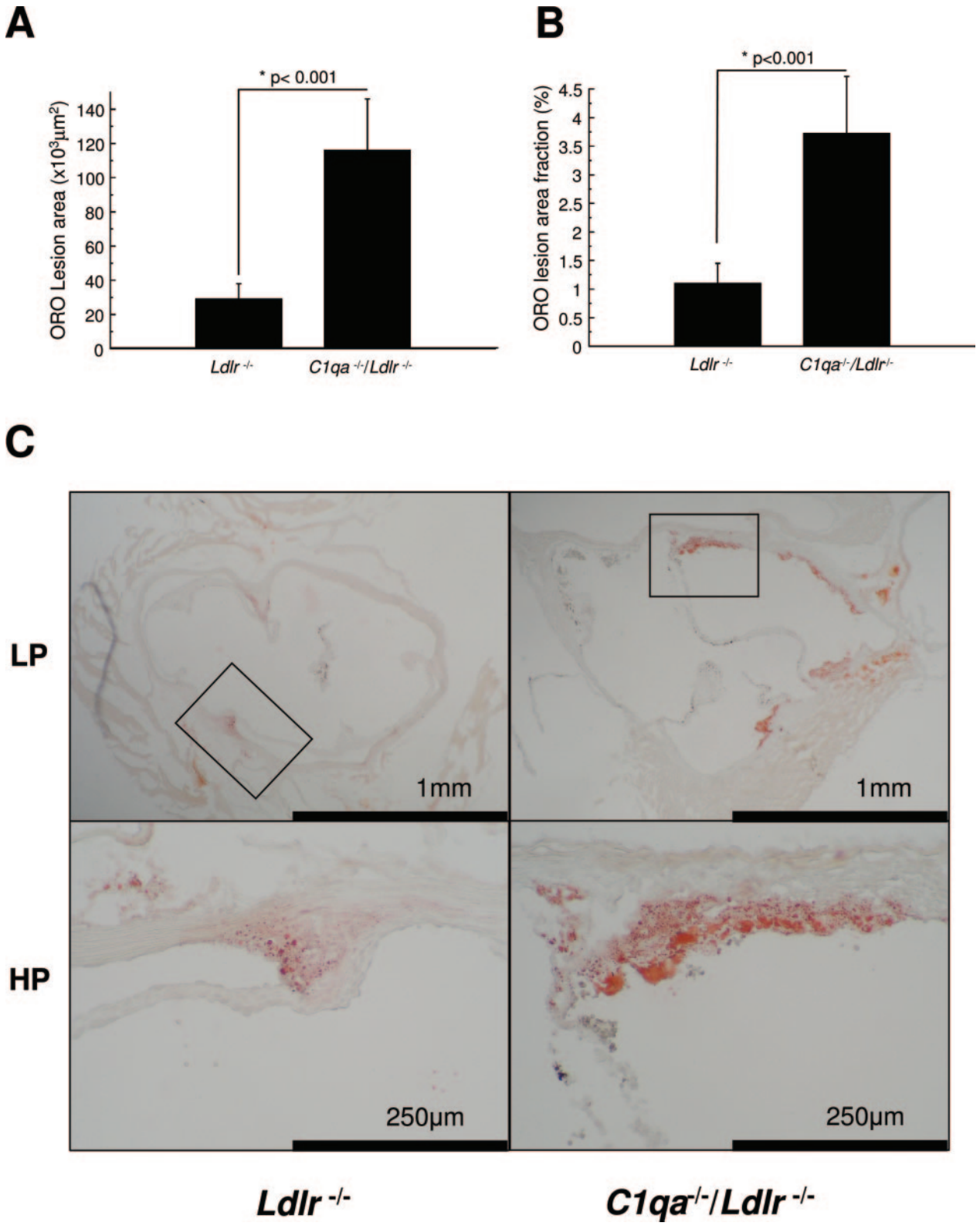

Figure 1. Increased aortic root lesion area in *C1qa*$^{-/-}$/*Ldlr*$^{-/-}$ mice. Comparison of lesion areas in *C1qa*$^{-/-}$/*Ldlr*$^{-/-}$ ($n = 8$) and *Ldlr*$^{-/-}$ ($n = 19$) animals after 22 weeks: (**A**) area of lesions stained by Oil Red O and hematoxylin, (**B**) % of vessel stained by Oil Red O and hematoxylin, and (**C**) photomicrographs of aortic roots at low power (LP) and high power (HP). The bars show the group means + SEM.

were postfixed in 4% glutaraldehyde at room temperature for 30 minutes. An area of interest was defined from the cleaved caspase-3 staining of the adjacent section. The relevant part of the section was then captured into a resin block. Semithin sections were used to confirm the local topography, after which the resin was ultramicrotomed

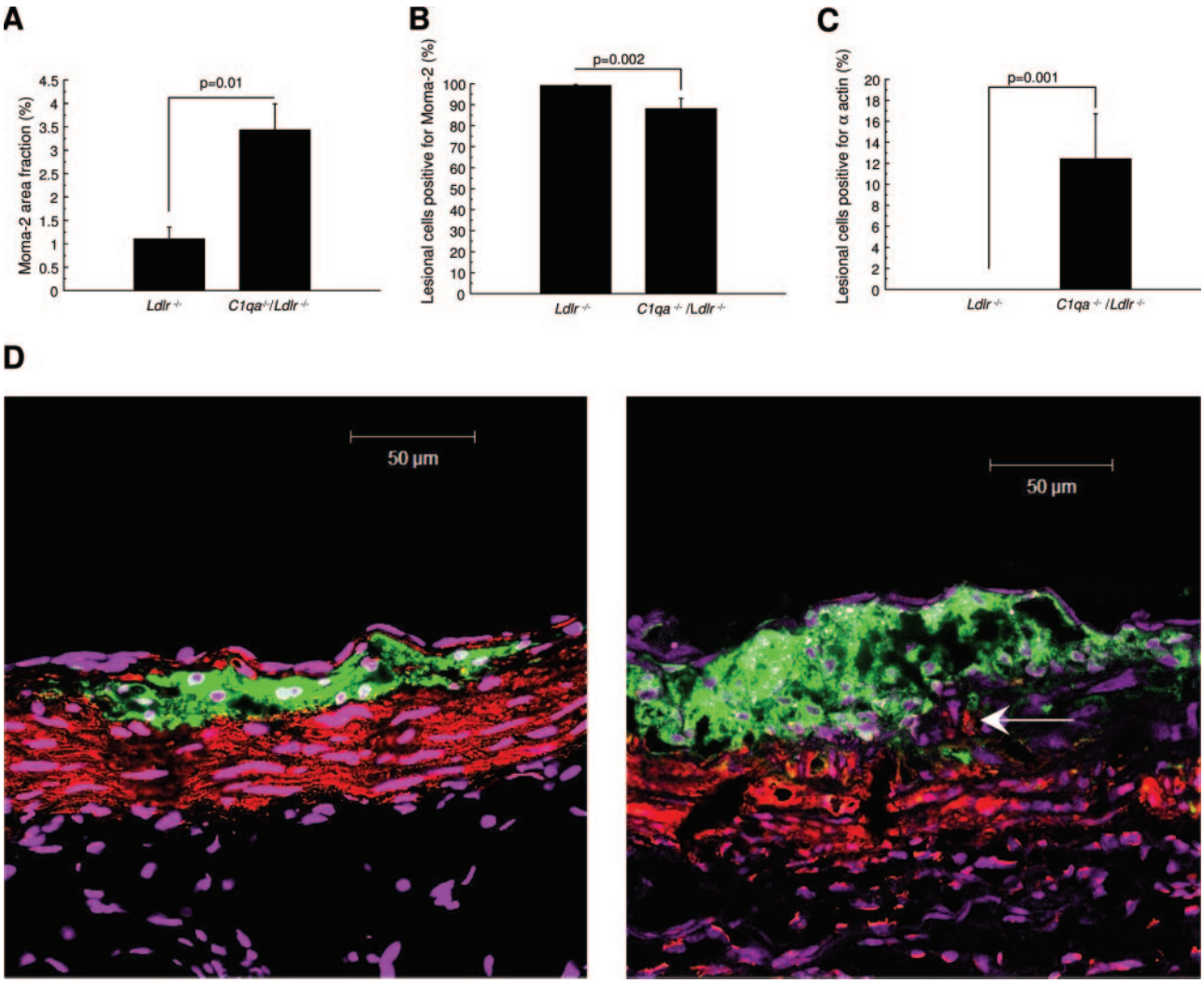

Figure 2. Increased complexity of aortic root lesions in $C1qa^{-/-}/Ldlr^{-/-}$ mice. Comparison of lesions in $C1qa^{-/-}/Ldlr^{-/-}$ ($n = 8$) and $Ldlr^{-/-}$ ($n = 19$) animals after 22 weeks: (**A**) percentage of vessel stained by Moma-2, (**B**) percentage of lesion cells stained by Moma-2, and (**C**) percentage of lesion cells staining positively for smooth muscle α-actin. Figure bars are group means + SEM. **D:** Confocal analysis of lesion complexity showing composite pseudocolored overlays. Aortic roots were double-immunostained with Moma-2 (Alexa488 detection) and anti-actin (Cy3 detection), together with a nuclear counterstain (TOPRO). The sections were mounted in PBS/glycerol and visualized using a Zeiss inverted confocal microscope. Purple, TOPRO (far red emission); red, Cy3 (orange/red emission); and green, Moma-2 (green emission). The **fine white arrow** in the right panel shows actin-positive VSMC (red) within a lesion surrounded by Moma-2-positive macrophages (green). This appearance was seen in lesions of $C1qa^{-/-}/Ldlr^{-/-}$ (right) but not $Ldlr^{-/-}$ (left) mice.

and ultrathin sections were stained with lead and imaged on a Hitachi 7650 transmission electron microscope (Hitachi Software Engineering, Yokohama, Japan) with digital capture. Because the cryostat-reprocessed tissue had low contrast staining, contrast was adjusted after acquisition in Adobe Photoshop (Adobe Systems, Mountain View, CA) in line with digital image guidelines.

Statistics

Data were expressed as mean ± SE unless otherwise stated and tested by one-tailed Student's *t*-test [Excel (Microsoft) and SigmaStat (Systat Software, Inc., Point Richmond, CA)], with significance assumed at $P < 0.05$.

Results

Mice were fed a normal laboratory diet or a high-fat diet from weaning until sacrifice at 22 weeks of age. As shown in Table 1, no differences were observed between $Ldlr^{-/-}$ and $C1qa^{-/-}/Ldlr^{-/-}$ strains for final body weight or for total serum cholesterol and triglyceride levels. Furthermore, there was no difference in the lipoprotein profile of $Ldlr^{-/-}$ and $C1qa^{-/-}/Ldlr^{-/-}$ mice, as determined by fast-performance liquid chromatography (FPLC) (not shown). No mouse of either strain had evidence of autoimmunity related to C1q deficiency, as shown by lack of proteinuria, the absence of glomerulonephritis, and the absence of antibodies to anti-ssDNA (not shown). Furthermore, there were no differences between $Ldlr^{-/-}$ and $C1qa^{-/-}$/

Ldlr$^{-/-}$ in the titers of antibodies to oxidatively modified lipoproteins (not shown).

In the first experiment, we analyzed lesion areas in aortic roots of *Ldlr*$^{-/-}$ and *C1qa*$^{-/-}$/*Ldlr*$^{-/-}$ mice fed a normal laboratory diet by standard methods and found that aortic root lesion areas were significantly greater in the *C1qa*$^{-/-}$/*Ldlr*$^{-/-}$ mice ($P < 0.006$, data not shown). We therefore performed a confirmatory experiment, in which we found that *C1qa*$^{-/-}$/*Ldlr*$^{-/-}$ mice had approximately threefold larger absolute lesion areas in the aortic root than *Ldlr*$^{-/-}$ animals (*C1qa*$^{-/-}$/*Ldlr*$^{-/-}$ 116 ± 30 × 10^3 μm^2 versus *Ldlr*$^{-/-}$ 28.8 ± 9.0 × 10^3 μm^2; mean ± SEM, $P < 0.001$) (Figure 1A). Furthermore, the lesion areas were also significantly increased in *C1qa*$^{-/-}$/*Ldlr*$^{-/-}$ mice when expressed as a fraction of the aortic root (*C1qa*$^{-/-}$/*Ldlr*$^{-/-}$ 3.72 ± 1.0% versus *LDLR*$^{-/-}$ 1.1 ± 0.4%; mean ± SEM, $P < 0.001$) (Figure 1B).

Lesions in *Ldlr*$^{-/-}$ mice fed a high-fat diet from 10 to 22 weeks of age were approximately 10-fold greater than those fed a normal laboratory diet, but, following a high-fat diet, there were no differences between *C1qa*$^{-/-}$/*Ldlr*$^{-/-}$ ($n = 10$) and *Ldlr*$^{-/-}$ ($n = 10$) mice in aortic root lesion area or fraction of the aortic occupied by lesions (lesion areas, *C1qa*$^{-/-}$/*Ldlr*$^{-/-}$ 443.34 ± 190.28 × 10^3 μm^2 versus *Ldlr*$^{-/-}$ 254.04 ± 75.28 × 10^3 μm^2; aortic root fraction, *C1qa*$^{-/-}$/*Ldlr*$^{-/-}$ 23.71 ± 7.61% versus *Ldlr*$^{-/-}$ 18.00 ± 5.63%). Subsequent analysis of lesions was therefore focused on mice fed a normal laboratory diet.

Staining of aortic root lesions with the macrophage marker Moma-2 highlighted cells with the features of foamy macrophages. The area of Moma-2 immunoreactive cells was significantly greater in *C1qa*$^{-/-}$/*Ldlr*$^{-/-}$ mice than from *Ldlr*$^{-/-}$ controls (area fraction of Moma-2-positive cells in *C1qa*$^{-/-}$/*Ldlr*$^{-/-}$ 3.3 ± 0.6% versus *Ldlr*$^{-/-}$ 1.1 ± 0.3%; mean ± SEM, $P = 0.01$) (Figure 2A). Whereas the cells in lesions of *Ldlr*$^{-/-}$ mice consisted exclusively of macrophages, lesions in *C1qa*$^{-/-}$/*Ldlr*$^{-/-}$ mice had ~12% of cells negative for Moma-2 (Figure 2, B and D) and positive for smooth muscle cell α-actin (Figure 2, C and D). We failed to detect B or T lymphocytes in lesions in either strain. There were no significant differences between strains in the proportion of lesions occupied by collagen, as detected using the Picrosirius Red method, or in immunohistochemical staining for IgG, IgM, or C3 (not shown).

Reactivity of anti-C5b-9 antibody, which was raised against human material, was established by showing that staining of aortic roots was abolished by prior absorption with IgM-coated polystyrene beads opsonized with normal human serum but not by IgM-coated beads opsonized with C3-deficient serum (not shown). C5b-9 staining in aortic root lesions of *Ldlr*$^{-/-}$ mice was identified particularly around lesional foam cells (Figure 3A). The percentage of aortic root lesions with positive C5b-9 staining was significantly less in *C1qa*$^{-/-}$/*Ldlr*$^{-/-}$ mice compared with *Ldlr*$^{-/-}$ mice (2.78 versus 24.6%; $P <$ 0.0001) (Figure 3, B and C).

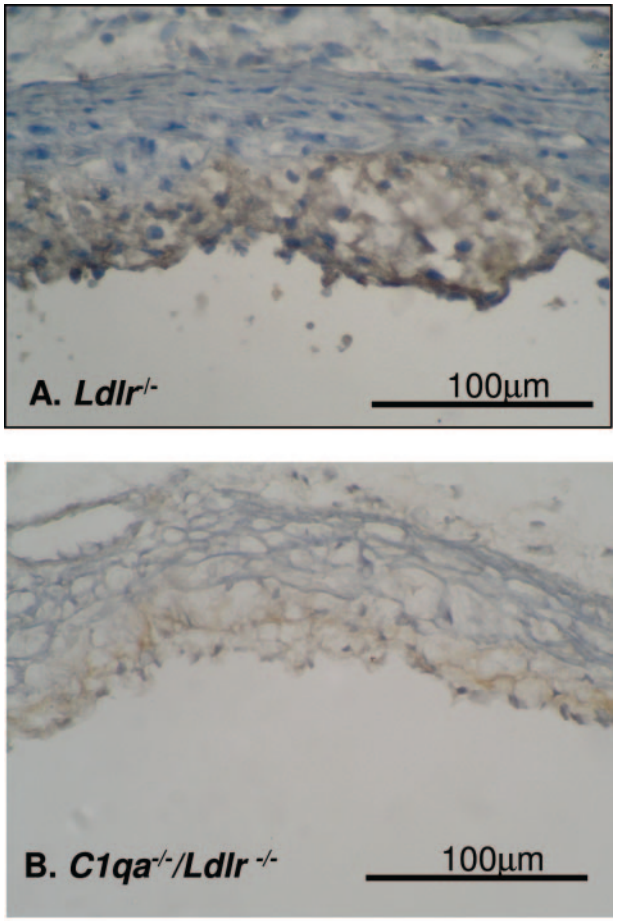

Figure 3. Deposition of C5b-9 in the aortic root. Photomicrograph of cryosections of aortic roots of (**A**) *Ldlr*$^{-/-}$ and (**B**) *C1qa*$^{-/-}$/*Ldlr*$^{-/-}$ mice stained with anti-C5b-9. C5b-9 deposition was seen diffusely around lesional foam cells; (**C**) shows a quantitative comparison between anti-C5b-9 staining of aortic roots of *Ldlr*$^{-/-}$ and *C1qa*$^{-/-}$/*Ldlr*$^{-/-}$ mice.

To quantify apoptotic cells, we performed immunohistochemical staining with an antibody against cleaved caspase-3. Lesions in *C1qa*$^{-/-}$/*Ldlr*$^{-/-}$ mice contained

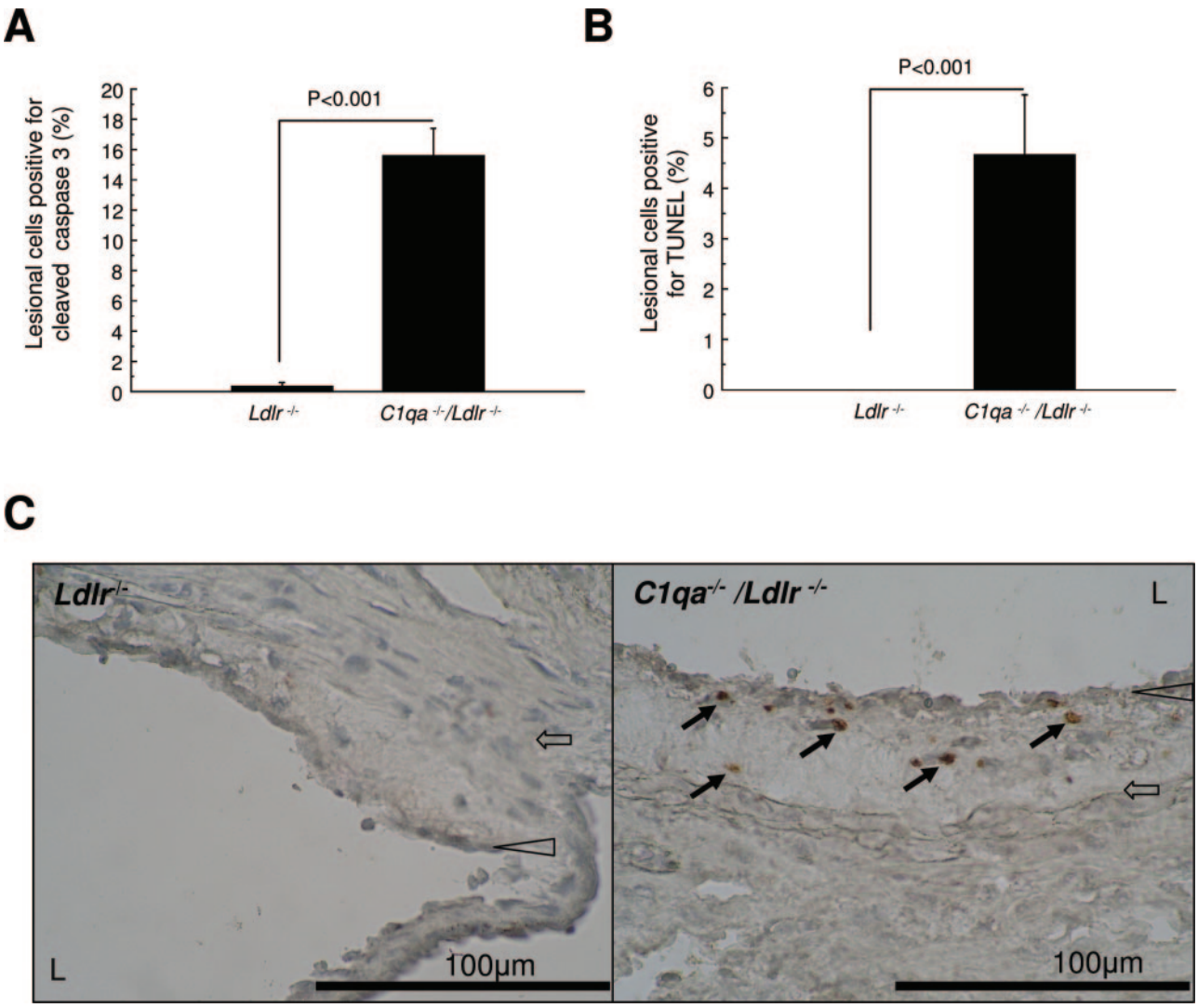

Figure 4. Increased apoptotic cells in aortic root lesions of $C1qa^{-/-}/Ldlr^{-/-}$ mice. Comparison of lesions in $C1qa^{-/-}/Ldlr^{-/-}$ ($n = 8$) and $Ldlr^{-/-}$ ($n = 19$) animals after 22 weeks: (**A**) percentage of plaque cells staining positively for cleaved caspase 3, (**B**) percentage of plaque cells staining positively by TUNEL, and (**C**) photomicrographs with **arrows** showing the absence and presence of cells staining positively for cleaved caspase-3 in $Ldlr^{-/-}$ mice (left panel) and $C1qa^{-/-}/Ldlr^{-/-}$ (right panel) mice, respectively. **Filled block arrows** point to apoptotic cells immunopositive for cleaved capsase-3. **Open arrowheads** point to the endothelial layer. L, lumen. **Open block arrows** point to the internal elastic lamina delimiting deep boundary of intima.

15.6 ± 1.8% cells (mean ± SEM) staining positively for activated caspase-3, whereas positive cells were barely detectable in the lesions of $Ldlr^{-/-}$ mice ($P < 0.001$) (Figure 4A). TUNEL staining confirmed the increase in apoptotic cells in $C1qa^{-/-}/Ldlr^{-/-}$ mice (4.7 ± 1.2 versus 0 ± 0 mean ± SEM % lesional cells) (Figure 4B). The number of TUNEL-positive cells was less than the number of cells stained by anti-caspase-3, at least in part due to anti-caspase-3 identifying cells at more stages of apoptosis than TUNEL.[30,31] It is also possible that our careful titration of the TUNEL reaction to avoid nonspecific labeling led to an underestimation of apoptotic cell number with this technique. No cells outside lesions stained positively in $C1qa^{-/-}/Ldlr^{-/-}$ for cleaved caspase-3 or by TUNEL. Double staining of lesions of $C1qa^{-/-}/Ldlr^{-/-}$ revealed the apoptotic cells to be macrophages (ie, Moma-2-positive and α-actin-negative) (Figure 5). The presence of apoptotic cells in aortic root lesions of $C1qa^{-/-}/Ldlr^{-/-}$ was confirmed by electron microscopy (Figure 6).

Discussion

In this study, we have explored the role of the classic complement pathway in atherosclerosis using C1q-deficient mice. We found that lesions in $C1qa^{-/-}/Ldlr^{-/-}$ mice at 22 weeks of age were approximately threefold larger and showed evidence of apoptotic macrophages and greater lesion complexity compared with those in $Ldlr^{-/-}$ animals. There were no differences in aortic root lesion size between $C1qa^{-/-}/Ldlr^{-/-}$ and $Ldlr^{-/-}$ strains when mice were fed a high-fat diet, suggesting that the classic complement pathway may play a particular role in limiting the size and complexity of early lesions.

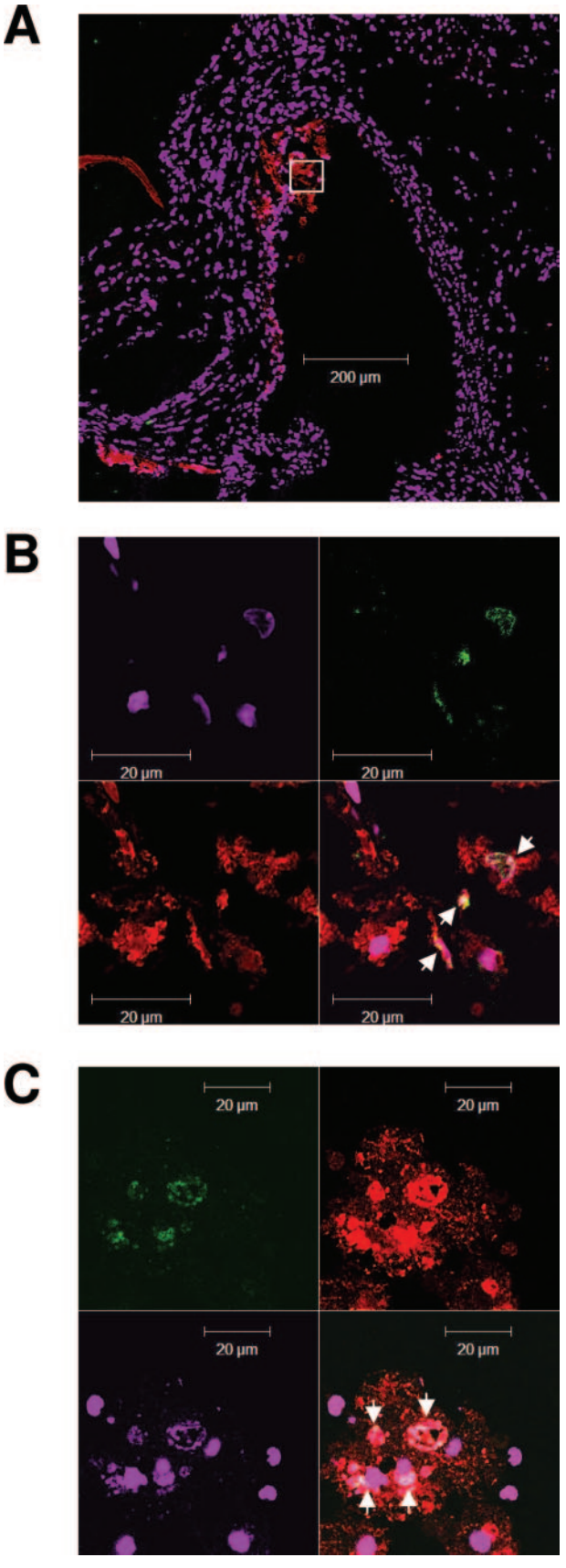

In both humans and mice, a consequence of C1q deficiency is the development of a systemic lupus erythematosus-like syndrome.[23,32] However, in mice this is dependent on genetic background, since *C1qa*$^{-/-}$ animals show no evidence of autoimmunity after backcrossing onto C57BL/6.[33] The mice in our study failed to develop proteinuria, glomerulonephritis, or anti-ssDNA and did not have altered titers of antibodies to oxidized lipoproteins, suggesting that our results were not related to the development of autoimmunity. Furthermore, we have also observed that *C1qa*$^{-/-}$ single knockout mice fail to develop autoimmunity when fed a high cholesterol/fat diet for 36 weeks (data not shown), indicating that elevated serum lipids are not sufficient to unmask autoimmunity in C1q-deficient mice in the absence of a susceptible genetic background. Likewise, we did not detect aortic root lesions in these *C1qa*$^{-/-}$ single knockout mice fed a high cholesterol/fat diet.

The greater aortic root lesion size in *C1qa*$^{-/-}$/*Ldlr*$^{-/-}$ mice occurred despite a significant reduction in C5b-9 deposition per lesion unit area, suggesting the critical importance of proximal pathway activity. A direct relation between C1q deficiency, failure to clear apoptotic cells, and increased lesion development is supported by the readily detectable presence of apoptotic cells in *C1qa*$^{-/-}$/*Ldlr*$^{-/-}$ mice but not in *Ldlr*$^{-/-}$ mice. The lack of detectable apoptotic cells in early lesions of *Ldlr*$^{-/-}$ single knockout has previously been reported.[34] We also found that *C1qa*$^{-/-}$/*Ldlr*$^{-/-}$ mice fed a normal laboratory diet up to 22 weeks have significantly more caspase-3-positive cells in aortic root lesions than *Ldlr* $^{-/-}$ mice fed a high-fat diet from weeks 10 to 22, despite having lesions ~2.5-fold smaller (not shown). This therefore suggests that the increase in apoptotic cells in *C1qa*$^{-/-}$/*Ldlr*$^{-/-}$ mice is not just related to lesion size. Because C1q deficiency is known to impair apoptotic cell clearance in other *in vivo* settings,[20,23] our data are consistent with a model in which apoptosis occurs in early lesions but is not normally detected because of highly efficient removal mechanisms. A proposed link between failure to clear apoptotic cells and accelerated lesion development has also recently been suggested in mice deficient in leukocyte transglutaminase 2.[35] Further work will be directed at determining the nature and roles in *C1qa*$^{-/-}$/*Ldlr*$^{-/-}$ mice of proinflammatory factors released or surface expressed on apoptotic cells, such as biologically active phospholipids.[36] Moreover, reduced apoptotic cell clearance may critically lower the release by macrophages of anti-inflammatory factors, such as transforming growth factor β (TGFβ), known to be expressed following apoptotic cell uptake.[37]

Figure 5. Double staining of apoptotic cells assessed by confocal microscopy. **A:** Low-power composite of cleaved caspase-3 (Alexa488, green), Moma-2 (Alexa 568, red), and TOPRO-3 nuclear dye (purple, pseudocolored; far red, original); (**B**) single channels of boxed area in **A**, with composite at bottom right. **White arrows** show cells triple-positive for TOPRO-3, Moma-2, and cleaved caspase-3; (**C**) equivalent of **B** in parallel section stained with Moma-2 (Alex 568, red) and TUNEL (FITC, green), with composite at bottom right. **White arrows** show cells triple-positive for TOPRO-3, TUNEL, and Moma-2. No such colocalization was seen on actin double staining (not shown, the resolution was less because the actin-positive cells were distant from the cleaved caspase-3-positive cells).

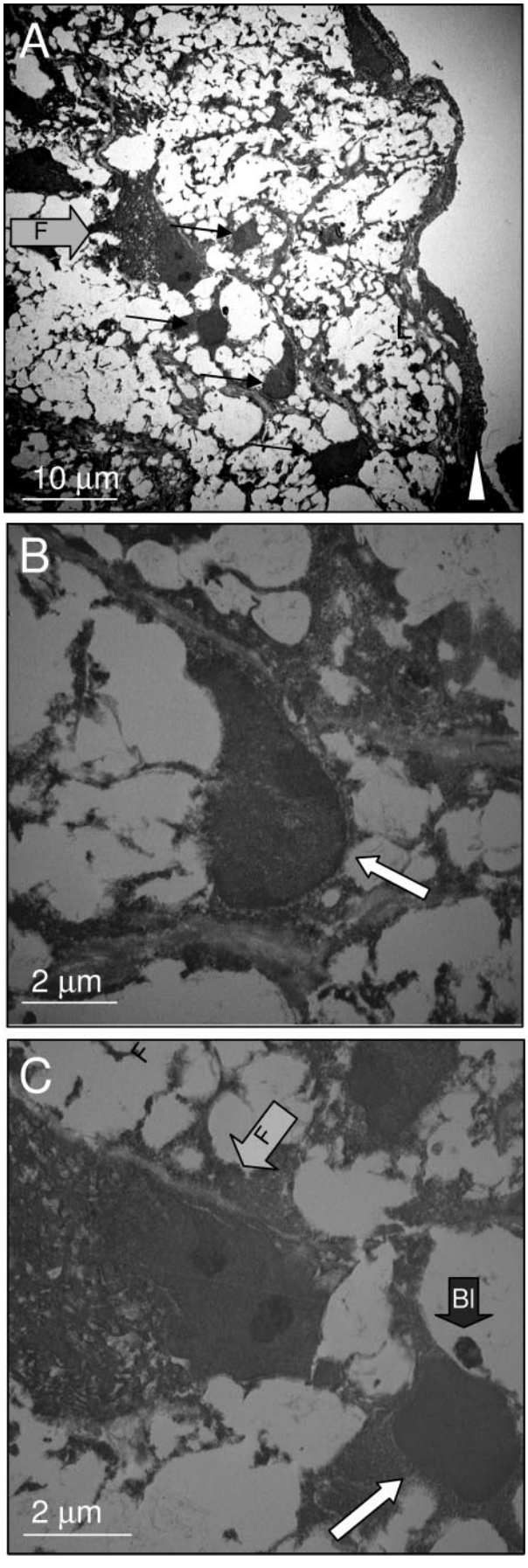

Our detection of C5b-9 in aortic root lesions of *Ldlr*$^{-/-}$ provides the first direct evidence for terminal complement pathway activation in a mouse atherosclerosis model and is consistent with studies in rabbit and human atherosclerosis.[38–41] C5b-9 deposition was significantly reduced in *C1qa*$^{-/-}$/*Ldlr*$^{-/-}$ mice, consistent with a major role of the classic pathway in driving C5b-9 generation. However, the presence of C5b-9 in the absence of apoptotic cells in *Ldlr*$^{-/-}$ mice shows that efficient disposal of apoptotic cells does not prevent C5b-9 formation. Furthermore, C5b-9 deposition was not completely abolished in the absence of C1q, suggesting involvement of the alternative and/or mannose-binding lectin pathways. In hyperlipidemic rabbits, C5b-9 deposition occurs at an early stage of atherogenesis in conjunction with cholesterol accumulation and, judging from protection in C6-deficient rabbit, seems to accelerate lesion formation.[40,42,43] Although C5b-9 is clearly generated in *Ldlr*$^{-/-}$ mice, it is important to note that fluid phase and cell surface inhibitors may act to reduce the amount of terminal pathway activation in relation to proximal pathway activity. Cell surface inhibitory factors, such as decay accelerating factor (CD55), CD59, and, in mice, complement receptor 1 (CR1)-related gene y (Crry) may be particularly important, because access of plasma inhibitors to the subendothelial space may be limited.[44] Preliminary observations in our group support this view, since we have found that aortic root lesions are significantly greater in *Ldlr*$^{-/-}$ mice deficient in CD59 (S. Yun, V. Leung, M. Botto, D. Haskard, J. Boyle, manuscript in preparation).

Our data should be viewed alongside previous studies on atherosclerosis in complement-deficient mice, although direct comparisons are not possible because of significant methodological differences. In particular, we have focused on early lesion development in mice fed a normal rodent diet. C3-deficient *Ldlr*$^{-/-}$ mice fed a high-cholesterol diet have been shown to have increased aortic lipid deposition after 15 weeks, with lesions containing more macrophages but fewer vascular smooth muscle cells.[45] A further study has reported an increase in aortic lesion area in *Ldlr*$^{-/-}$/*ApoE*$^{-/-}$ double knockout mice deficient in C3, but it should be noted that these mice had a more atherogenic lipid profile.[46] In the same study, impairment of the alternative pathway because of factor B deficiency had no influence on lesion development.[46] Last, Patel and colleagues found no effect of reduced downstream complement activity because of C5 deficiency in *ApoE*$^{-/-}$ mice.[47] A role for the MBL pathway in mouse atherosclerosis remains possible, given the in-

Figure 6. Apoptotic cells in EM aortic root lesions of *C1qa*$^{-/-}$/*Ldlr*$^{-/-}$ mice. **A:** Low magnification for orientation. L, lumen. **White arrowhead** points to endothelial layer. **Fine arrows** point to apoptotic cells, identified by characteristic electron dense peripheral chromatin condensation. **B** and **C** are higher magnifications. **Gray-filled block arrows** marked with F, foam cell(s). In **B,** the **white block arrow** points to a shrunken cell with characteristic electron dense peripheral chromatin condensation and cytoplasmic collapse, characteristic of apoptosis; in **C**, the **white block arrow** points to an early apoptotic cell with early electron dense peripheral chromatin condensation and characteristic blebbing, containing electron dense material (Bl, white script within filled **black block arrow**). **Gray-filled block arrow** with F, foam cell.

volvement of MBL in apoptotic cell clearance[22,48] and also the suggested link between MBL deficiency and atherosclerosis in humans.[49] In summary, our investigation shows for the first time that the classic pathway of complement activation is involved in atherosclerosis, with C1q providing a protective function, possibly by accelerating the clearance of apoptotic cells.

Acknowledgments

We thank the British Heart Foundation and Hammersmith Hospitals NHS Trust Research Committee for financial support. We thank Dr. Joseph Witztum (University of California San Diego, La Jolla) for the analysis of antibodies to modified lipoproteins. We also thank Dr. Clare Roberts (BHF Cardiovascular Medicine Unit) and Ms. Yolande Sadler, Mr. Ian Shore, and Dr. Jill Moss (Histopathology, Hammersmith Hospital) for advice and technical support.

References

1. Walport MJ: Complement. First of two parts. N Engl J Med 2001, 344:1058–1066
2. Walport MJ: Complement. Second of two parts. N Engl J Med 2001, 344:1140–1144
3. Niculescu F and Rus H: Mechanisms of signal transduction activated by sublytic assembly of terminal complement complexes on nucleated cells. Immunol Res 2001, 24:191–199
4. Mevorach D, Mascarenhas JO, Gershov D, and Elkon KB: Complement-dependent clearance of apoptotic cells by human macrophages. J Exp Med 1998, 188:2313–2320
5. Gershov D, Kim S, Brot N, and Elkon KB: C-Reactive protein binds to apoptotic cells, protects the cells from assembly of the terminal complement components, and sustains an antiinflammatory innate immune response: implications for systemic autoimmunity. J Exp Med 2000, 192:1353–1364
6. Fishelson Z, Attali G, and Mevorach D: Complement and apoptosis. Mol Immunol 2001, 38:207–219
7. Han DKM, Hauderschild CC, Hong MK, Tinkle BT, Leon MB, Liau G: Evidence for apoptosis in human atherogenesis and in a rat vascular injury model. Am J Pathol 1995, 147:267–277
8. Björkerud S, Björkerud B: Apoptosis is abundant in human atherosclerotic lesions, especially in inflammatory cells (macrophages and T cells), and may contribute to the accumulation of gruel and plaque instability. Am J Pathol 1996, 149:367–380
9. Mallat Z, Ohan J, Leseche G, Tedgui A: Colocalization of CPP-32 with apoptotic cells in human atherosclerotic plaques. Circulation 1997, 96:424–428
10. Yao PM, Tabas I: Free cholesterol loading of macrophages induces apoptosis involving the fas pathway. J Biol Chem 2000, 275:23807–23813
11. Tabas I: Consequences of cellular cholesterol accumulation: basic concepts and physiological implications. J Clin Invest 2002, 110:905–911
12. Carpenter KL, Challis IR, Arends MJ: Mildly oxidised LDL induces more macrophage death than moderately oxidised LDL: roles of peroxidation, lipoprotein-associated phospholipase A2 and PPAR-gamma. FEBS Lett 2003, 553:145–150
13. Niemann-Jönsson A, Ares MP, Yan ZQ, Bu DX, Fredrikson GN, Branen L, Porn-Ares I, Nilsson AH, Nilsson J: Increased rate of apoptosis in intimal arterial smooth muscle cells through endogenous activation of TNF receptors. Arterioscler Thromb Vasc Biol 2001, 21:1909–1914
14. Boyle JJ, Weissberg PL, Bennett MR: Human macrophage-induced vascular smooth muscle cell apoptosis requires NO enhancement of Fas/Fas-L interactions. Arterioscler Thromb Vasc Biol 2002, 22:1624–1630
15. Loidl A, Sevcsik E, Riesenhuber G, Deigner HP, Hermetter A: Oxidized phospholipids in minimally modified low density lipoprotein induce apoptotic signaling via activation of acid sphingomyelinase in arterial smooth muscle cells. J Biol Chem 2003, 278:32921–32928
16. Kockx MM: Apoptosis in the atherosclerotic plaque: quantitative and qualitative aspects. Arterioscler Thromb Vasc Biol 1998, 18:1519–1522
17. Tabas I: Consequences and therapeutic implications of macrophage apoptosis in atherosclerosis: the importance of lesion stage and phagocytic efficiency. Arterioscler Thromb Vasc Biol 2005, 25:2255–2264
18. Korb LC, Ahearn JM: C1q binds directly and specifically to surface blebs of apoptotic human keratinocytes: complement deficiency and systemic lupus erythematosus revisited. J Immunol 1997, 158:4525–4528
19. Navratil JS, Watkins SC, Wisnieski JJ, Ahearn JM: The globular heads of C1q specifically recognize surface blebs of apoptotic vascular endothelial cells. J Immunol 2001, 166:3231–3239
20. Taylor PR, Carugati A, Fadok VA, Cook HT, Andrews M, Carroll MC, Savill JS, Henson PM, Botto M, Walport MJ: A hierarchical role for classical pathway complement proteins in the clearance of apoptotic cells in vivo. J Exp Med 2000, 192:359–366
21. Nauta AJ, Trouw LA, Daha MR, Tijsma O, Nieuwland R, Schwaeble WJ, Gingras AR, Mantovani A, Hack EC, Roos A: Direct binding of C1q to apoptotic cells and cell blebs induces complement activation. Eur J Immunol 2002, 32:1726–1736
22. Ogden CA, deCathelineau A, Hoffmann PR, Bratton D, Ghebrehiwet B, Fadok VA, Henson PM: C1q and mannose binding lectin engagement of cell surface calreticulin and CD91 initiates macropinocytosis and uptake of apoptotic cells. J Exp Med 2001, 194:781–795
23. Botto M, Dell'Agnola C, Bygrave AE, Thompson EM, Cook HT, Petry F, Loos M, Pandolfi P, Walport MJ: Homozygous C1q deficiency causes glomerulonephritis associated with multiple apoptotic bodies. Nat Genet 1998, 19:56–59
24. Benson GM, Schiffelers R, Nicols C, Latcham J, Vidgeon-Hart M, Toseland CD, Suckling KE, Groot PH: Effect of probucol on serum lipids, atherosclerosis and toxicology in fat-fed LDL receptor deficient mice. Atherosclerosis 1998, 141:237–247
25. Burlingame RW, Rubin RL: Subnucleosome structures as substrates in enzyme-linked immunosorbent assays. J Immunol Methods 1990, 134:187–199
26. Tsimikas S, Palinski W, Witztum JL: Circulating autoantibodies to oxidized LDL correlate with arterial accumulation and depletion of oxidized LDL in LDL receptor-deficient mice. Arterioscler Thromb Vasc Biol 2001, 21:95–100
27. Paigen B, Morrow A, Holmes PA, Mitchell D, Williams RA: Quantitative assessment of atherosclerotic lesions in mice. Atherosclerosis 1987, 68:231–240
28. Groot PH, van Vlijmen BJ, Benson GM, Hofker MH, Schiffelers R, Vidgeon-Hart M, Havekes LM: Quantitative assessment of aortic atherosclerosis in APOE*3 Leiden transgenic mice and its relationship to serum cholesterol exposure. Arterioscler Thromb Vasc Biol 1996, 16:926–933
29. Robertson AK, Rudling M, Zhou X, Gorelik L, Flavell RA, Hansson GK: Disruption of TGF-beta signaling in T cells accelerates atherosclerosis. J Clin Invest 2003, 112:1342–1350
30. Belloc F, Belaud-Rotureau MA, Lavignolle V, Bascans E, Braz-Pereira E, Durrieu F, Lacombe F: Flow cytometry detection of caspase 3 activation in preapoptotic leukemic cells. Cytometry 2000, 40:151–160
31. Duan WR, Garner DS, Williams SD, Funckes-Shippy CL, Spath IS, Blomme EA: Comparison of immunohistochemistry for activated caspase-3 and cleaved cytokeratin 18 with the TUNEL method for quantification of apoptosis in histological sections of PC-3 subcutaneous xenografts. J Pathol 2003, 199:221–228
32. Walport MJ, Davies KA, Botto M: C1q and systemic lupus erythematosus. Immunobiology 1998, 199:265–285
33. Mitchell DA, Pickering MC, Warren J, Fossati-Jimack L, Cortes-Hernandez J, Cook HT, Botto M, Walport MJ: C1q deficiency and autoimmunity: the effects of genetic background on disease expression. J Immunol 2002, 168:2538–2543
34. Harada K, Chen Z, Ishibashi S, Osuga J, Yagyu H, Ohashi K, Yahagi N, Shionoiri F, Sun L, Yazaki Y, Yamada N: Apoptotic cell death in atherosclerotic plaques of hyperlipidemic knockout mice. Atherosclerosis 1997, 135:235–239
35. Boisvert WA, Rose DM, Boullier A, Quehenberger O, Sydlaske A,

Johnson KA, Curtiss LK, Terkeltaub R: Leukocyte transglutaminase 2 expression limits atherosclerotic lesion size. Arterioscler Thromb Vasc Biol 2006, 26:563–569
36. Kadl A, Bochkov VN, Huber J, Leitinger N: Apoptotic cells as sources for biologically active oxidized phospholipids. Antioxid Redox Signal 2004, 6:311–320
37. Fadok VA, Bratton DL, Konowal A, Freed PW, Westcott JY, Henson PM: Macrophages that have ingested apoptotic cells in vitro inhibit proinflammatory cytokine production through autocrine/paracrine mechanisms involving TGF-beta, PGE2, and PAF. J Clin Invest 1998, 101:890–898
38. Niculescu F, Rus H, Cristea A, Vlaicu R: Localization of the terminal C5b-9 complement complex in the human aortic atherosclerotic wall. Immunol Lett 1985, 10:109–114
39. Rus HG, Niculescu F, Vlaicu R: Co-localization of terminal C5b-9 complement complexes and macrophages in human atherosclerotic arterial walls. Immunol Lett 1988, 19:27–32
40. Seifert PS, Hugo F, Hansson GK, Bhakdi S: Prelesional complement activation in experimental atherosclerosis. Terminal C5b-9 complement deposition coincides with cholesterol accumulation in the aortic intima of hypercholesterolemic rabbits. Lab Invest 1989, 60:747–754
41. Torzewski M, Torzewski J, Bowyer DE, Waltenberger J, Fitzsimmons C, Hombach V, Gabbert HE: Immunohistochemical colocalization of the terminal complex of human complement and smooth muscle cell alpha-actin in early atherosclerotic lesions. Arterioscler Thromb Vasc Biol 1997, 17:2448–2452
42. Geertinger P, Sørensen H: On the reduced atherogenic effect of cholesterol feeding in rabbits with congenital complement (C6) deficiency. Artery 1977, 1:177–184
43. Schmiedt W, Kinscherf R, Deigner HP, Kamencic H, Nauen O, Kilo J, Oelert H, Metz J, Bhakdi S: Complement C6 deficiency protects against diet-induced atherosclerosis in rabbits. Arterioscler Thromb Vasc Biol 1998, 18:1790–1795
44. Oksjoki R, Jarva H, Kovanen PT, Laine P, Meri S, Pentikainen MO: Association between complement factor H and proteoglycans in early human coronary atherosclerotic lesions: implications for local regulation of complement activation. Arterioscler Thromb Vasc Biol 2003, 23:630–636
45. Buono C, Come CE, Witztum JL, Maguire GF, Connelly PW, Carroll M, Lichtman AH: Influence of C3 deficiency on atherosclerosis. Circulation 2002, 105:3025–3031
46. Persson L, Boren J, Robertson AK, Wallenius V, Hansson GK, Pekna M: Lack of complement factor C3, but not factor B, increases hyperlipidemia and atherosclerosis in Apolipoprotein E−/− low-density lipoprotein receptor−/− mice. Arterioscler Thromb Vasc Biol 2004, 24:1062–1067
47. Patel S, Thelander EM, Hernandez M, Montenegro J, Hassing H, Burton C, Mundt S, Hermanowski-Vosatka A, Wright SD, Chao YS, Detmers PA: ApoE(−/−) mice develop atherosclerosis in the absence of complement component C5. Biochem Biophys Res Commun 2001, 286:164–170
48. Stuart LM, Takahashi K, Shi L, Savill J, Ezekowitz RA: Mannose-binding lectin-deficient mice display defective apoptotic cell clearance but no autoimmune phenotype. J Immunol 2005, 174:3220–3226
49. Madsen HO, Videm V, Svejgaard A, Svennevig JL, Garred P: Association of mannose-binding-lectin deficiency with severe atherosclerosis. Lancet 1998, 352:959–960